AD-A252 882

‖‖‖‖‖‖‖‖‖‖‖‖‖‖

EOS ①

Electro-Optical Sciences Inc.
1 Bridge Street
Irvington-on-Hudson, NY 10533
Tel #:   914/591-3783
Fax #:   914/591-3785

11 June 1992

DRAFT FINAL REPORT
(CDRL A002)

Contract N00014-90-C-0215

Multiangle Lidar Performance in the Presence of Horizontal Inhomogeneities in Atmospheric Extinction and Scattering

DTIC
S ELECTE
JUL 16 1992
A D

Authored by:

Dina Gutkowicz-Krusin

Electro-Optical Sciences, Inc.
1 Bridge Street
Irvington, NY 10533

Prepared for:

Robert Mongeon
Office of Naval Research
495 Summer Street
Boston, MA 02210

EOS/FR-0215

92-16478
‖‖‖‖‖‖‖‖‖‖‖‖‖

92 6 2 003

EOS

ABSTRACT

The performance of the single-ended multiangle lidar for measurements of atmospheric extinction and backscattering is analyzed in the presence of signal-induced shot noise. An algorithm for determining the transmission coefficient in the presence of horizontal inhomogeneities is described. The analysis indicates that real-time measurements of atmospheric properties with the multiangle lidar may be feasible even in inhomogeneous regions.

Accesion For		
NTIS CRA&I		☑
DTIC TAB		☐
Unannounced		☐
Justification		
By		
Distribution /		
Availability Codes		
Dist	Avail a..d / or Special	
A-1		

Statement A per telecon Mathew White
ONR/Code 126
Arlington, VA 22217-5000
NWW 7/15/82

TABLE OF CONTENTS

LIST OF FIGURES

1. Introduction

Since the aerosol constituents of the atmosphere can be highly variable, it is important to have the means to determine the atmospheric extinction and backscattering coefficients in real time. Remote sensing lidars are the most promising instruments for such measurements.[1] Typically, remote sensing lidars require *ad hoc* assumptions about the relationship between extinction and backscattering in order to determine the transmission coefficient from the range-resolved lidar returns. It is of course desirable to determine the transmission coefficient from lidar data without assuming any such relationships. Several methods to achieve this have been proposed: the Doppler lidar,[2,3] the bipath lidar,[4,5] and the multiangle lidar.[6-10]

The Doppler lidar[2,3] uses differences in the thermal Doppler broadening of radiation backscattered by molecules and aerosols to determine their respective contributions to the overall measured lidar return. The transmission coefficient is then calculated by comparing the measured molecular contribution to that predicted by the standard atmospheric models.

The bipath method employs two separate, single-ended lidar systems to measure both the backscattering and extinction coefficients unambiguously.[4,5] Hughes and Paulson[5] have shown that the backscattering and extinction coefficients obtained from a single lidar using typical *a priori* assumptions (i.e, Klett's reconstruction algorithm[11,12]) were significantly different from the values obtained with the bipath lidar. However, while elegant, the bipath lidar is difficult to use as a function of altitude.

In this paper, the performance of a single-ended multiangle lidar for real-time measurements of atmospheric transmission and backscattering is discussed. This lidar utilizes the dependence of the atmospheric transmission coefficient on the zenith angle, to obtain two independent equations for the backscattering and transmission coefficients from measurements along two paths with different zenith angles. Therefore, no *ad hoc* assump-

tions about the aerosol extinction and backscattering coefficients are required in order to determine these coefficients as functions of altitude.

Lidar measurements of atmospheric extinction and backscattering as a function of the zenith angle have been carried out in the past by Spinhirne et al.[7] Their data indicate that at the time of measurements the atmosphere was horizontally homogeneous above 3 km, but inhomogeneous in the boundary layer. This is not surprising since these data were collected at widely spaced intervals of the zenith angle (which was varied from 0° to about 80°).

Similar measurements were attempted by Paulson,[8] who collected lidar returns from optical paths with elevation angles of 25 and 50°. Even though the atmosphere was not horizontally homogeneous for such large angular separations, no attempt to vary the elevation angles was made.

Successful determinations of transmission coefficient from the lidar returns collected for different zenith angles were reported by Sandford[9] and Shimizu et al.[10] These results suggest that the uncertainty in the values of the aerosol extinction and backscattering obtained by Spinhirne et al.[7] and Paulson[8] could be considerably reduced by utilizing only the returns from optical paths with angular separation smaller than the angular size of horizontal inhomogeneities. In the multiangle lidar discussed here, this angular separation can be determined in real time by comparing returns obtained for a fixed zenith angle, but different azimuth angles of the optical paths. The minimum angular separation of the paths, based on noise considerations, is discussed in Sec. 2. An algorithm to determine the extinction and backscattering coefficients in the horizontally inhomogeneous region is described in Sec. 3. Results of calculations using this algorithm are presented in Sec. 4 and conclusions in Sec. 5.

2. Multiangle Lidar Performance in a Horizontally Homogeneous Atmosphere

Consider a standard lidar pointed along a LOS with zenith angle θ. The lidar equation

can be written as[1]

$$E(z,\theta) = \frac{C}{z^2} \cos^2\theta \, \beta(z,\theta) \exp\left[-\frac{2}{\cos\theta}\int_0^z dz' \, k_{ext}(z',\theta)\right] , \qquad (1)$$

where E is the average energy of radiation backscattered from the range $R = z/\cos\theta$, C is the calibration constant, and β and k_{ext} are the volume backscattering and extinction coefficients, respectively.

Consider two lines-of-sight with zenith angles θ and $\theta + \Delta\theta$, respectively. Assuming that the atmosphere is horizontally homogeneous over the angular separation $\Delta\theta$, the two-way transmission coefficient as a function of range can be obtained from the lidar signals obtained for zenith angles θ and $\theta + \Delta\theta$

$$T(R = z/\cos\theta) \equiv \exp\left[-\frac{2}{\cos\theta}\int_0^z dz' \, k_{ext}(z',\theta)\right] = [Q(z)]^\gamma \qquad (2)$$

where

$$\gamma = \frac{\cos(\theta + \Delta\theta)}{\cos(\theta + \Delta\theta) - \cos\theta} , \qquad (3)$$

and

$$Q(z) \equiv \frac{E(z/\cos\theta)}{E(z/\cos(\theta + \Delta\theta))} \frac{\cos^2(\theta + \Delta\theta)}{\cos^2\theta} . \qquad (4)$$

Since $Q(z)$ depends only on the ratio of the received signals, the transmission coefficient can be determined without absolute calibration of the lidar. This is also the case for the extinction coefficient which is given by

$$k_{ext}(z) = -\frac{1}{2}\gamma \cos(\theta) \frac{\partial}{\partial z} \ln Q(z) . \qquad (5)$$

However, absolute calibration of the lidar is still required in order to determine the volume backscattering coefficient β from the lidar equation (1).

Since γ increases with decreasing angular separation between the two optical paths, there must be a minimum value of $\Delta\theta$, or maximum value of γ, in order to obtain reliable results in the presence of noise. The performance degradation of the multiangle lidar due to signal-induced shot noise is discussed below.

Let $N_k(z, \theta)$ be the number of photocounts detected by the lidar receiver from altitude z along the optical path with zenith angle θ for the kth pulse. If turbulence effects are neglected, the probability of detecting such a number of photocounts is governed by Poisson statistics, i.e., the probability density function is

$$p(N_k) = \frac{(N_s + N_b)^{N_k}}{N_k!} e^{-(N_s + N_b)}, \tag{6}$$

where N_s and N_b are the expected numbers of signal and background photocounts, respectively. The expected value and variance of the detected photocounts are:

$$< N_k > = N_s + N_b, \tag{7}$$

$$\sigma_N^2 = < N_k^2 > - < N_k >^2 = N_s + N_b. \tag{8}$$

In order to reduce the variance in the measurements, consider a sum of random variables N_k:

$$n = \frac{1}{K} \sum_{k=1}^{K} N_k, \tag{9}$$

where K is the number of laser pulses used in averaging. Then, for $K \to \infty$, the central limit theorem gives the probability density function for n:[12]

$$p(n) = \left[\frac{K}{2\pi(N_s + N_b)} \right]^{1/2} \exp \left[-K \frac{(n - N_s - N_b)^2}{2(N_s + N_b)} \right]. \tag{10}$$

The corresponding expectation value and variance are:

$$< n > = N_s + N_b, \tag{11}$$

$$\sigma_n^2 = (N_s + N_b)/K. \tag{12}$$

The purpose of the measurements is to determine the two-way transmission coefficient from the ground to altitude z along the optical path with zenith angle θ. Let n_1 and n_2 be the average numbers of photocounts from altitude z for the optical paths with zenith angles

$\theta + \Delta\theta$ and θ, respectively. Then, assuming that horizontal gradients in backscattering and extinction coefficients can be neglected, the transmission coefficient is

$$T(z,\theta) = A^\gamma \left(\frac{n_1 - N_{b1}}{n_2 - N_{b2}} \right)^\gamma, \qquad (13)$$

where

$$A = \frac{\cos^2(\theta)}{\cos^2(\theta + \Delta\theta)} \qquad (14)$$

and

$$\gamma = \frac{\cos(\theta + \Delta\theta)}{\cos(\theta) - \cos(\theta + \Delta\theta)}. \qquad (15)$$

Since n_1 and n_2 are independent random variables, the expectation value and variance of T can be written as:

$$< T > = A^\gamma I_\gamma(N_{s1}, N_{b1}, K_1) I_{-\gamma}(N_{s2}, N_{b2}, K_2), \qquad (16)$$

and

$$\sigma_T^2 = A^{2\gamma}[I_{2\gamma}(N_{s1}, N_{b1}, K_1) I_{-2\gamma}(N_{s2}, N_{b2}, K_2) - I_\gamma^2(N_{s1}, N_{b1}, K_1) I_{-\gamma}^2(N_{s2}, N_{b2}, K_2)], \qquad (17)$$

where

$$I_\alpha(N_s, N_b, K) = \left[\frac{K}{2\pi(N_s + N_b)} \right]^{1/2} \int_{N_b + \epsilon N_s}^\infty dn \, (n - N_b)^\alpha \exp\left[-K \frac{(n - N_s - N_b)^2}{2(N_s + N_b)} \right]. \qquad (18)$$

A small positive value of ϵ (e.g., $\epsilon = 0.01$) is introduced in order to avoid artificial singularities for negative values of α if $n = N_b$. Clearly, in the absence of signal no useful information about the transmission coefficient can be obtained from the measurements.

It should be noted that the range of integration in Eq. (18) is such that the values of $n < N_b + \epsilon N_s$ are excluded. This is a very good approximation since the probability of n in this range is less than 0.5% for $KN_s^2/(N_s + N_b) \geq 5$. As will be seen later, the condition $KN_s^2/(N_s + N_b) \gg 5$ must be satisfied in order to obtain reliable values of the transmission coefficient.

In general, the integrals in Eq.(17) must be evaluated numerically. However, in the limit $K \to \infty$, these integrals can be estimated analytically. Eq. (18) may be rewritten

$$I_\alpha(N_s, N_b, K) = \frac{N_s^\alpha}{\sqrt{\pi}} \int_{-(1-\epsilon)\delta}^{\infty} dz \left(1 + \frac{z}{\delta}\right)^\alpha e^{-z^2} \qquad (19)$$

where

$$\delta^2 = \frac{K N_s^2}{2(N_s + N_b)}. \qquad (20)$$

For $\delta \gg 1$ we have

$$I_\alpha(N_s, N_b, K) = N_s^\alpha \sum_{n=0}^{\infty} \frac{a_{2n}(2n-1)!!}{2^n \delta^{2n}} + O(e^{-\delta^2}), \qquad (21)$$

where

$$a_0 = 1,$$

$$a_n = \alpha(\alpha-1)\cdots(\alpha-n+1)/n!, \quad n \geq 1. \qquad (22)$$

Therefore, the relative error in the value of the transmission coefficient obtained with the multiangle lidar is

$$\frac{\sigma_T^2}{<T>^2} = \gamma^2 \left[\frac{N_{s1} + N_{b1}}{K_1 N_{s1}^2} + \frac{N_{s2} + N_{b2}}{K_2 N_{s2}^2} \right]$$

$$+ \frac{\gamma^2(\gamma-1)(3\gamma-5)(N_{s1} + N_{b1})^2}{2K_1^2 N_{s1}^4}$$

$$\qquad (23)$$

$$+ \frac{\gamma^2(\gamma+1)(3\gamma+5)(N_{s2} + N_{b2})^2}{2K_2^2 N_{s2}^4}$$

$$+ \frac{3\gamma^4(N_{s1} + N_{b1})(N_{s2} + N_{b2})}{2K_1 K_2 N_{s1}^2 N_{s2}^2} + O(\delta^{-6}).$$

Expression (23) is useful for estimating the number of laser pulses K_1 and K_2 required to obtain the desired accuracy in transmission measurements, given the signal and background levels along the two optical paths. It can also be used to determine the maximum

allowed value of γ, i.e., the minimum angular separation between the optical paths, if other parameters are fixed.

The characteristic length scale of horizontal inhomogeneity can be determined by the multiangle lidar in real time by collecting returns for a fixed zenith angle and different azimuth angle. For a horizontally homogeneous atmosphere the lidar return should be independent of the azimuth angle ϕ. In practice, this can be tested by comparing the range-resolved lidar returns from optical paths separated by $\Delta\phi$, taking into account the uncertainties of individual returns. If the atmosphere is not homogeneous, the separation in azimuth angle could be decreased, until the locally homogeneous region has been found. If the corresponding separation in the zenith angle is less than the minimum separation allowed by the noise considerations, then it may become necessary to use a different approach. An algorithm designed to perform in the presence of inhomogeneities is described in the following section.

3. An Algorithm to Determine Extinction and Backscattering in a Horizontally Inhomogeneous Atmosphere

In the derivation of the transmission coefficient from the lidar returns for two optical paths with zenith angles θ and $\theta + \Delta\theta$ it has been assumed that the backscattering and extinction coefficients are functions of altitude only. Consider now a situation when this assumption is not valid.

From Eq. (1), for a fixed azimuth angle, the range-corrected lidar return from the optical path with the zenith angle θ is

$$F(z,\theta) = C\,\beta(z,\theta)\,\exp\left[-\frac{2}{\cos\theta}\int_0^z dz'\,k_{ext}(z',\theta)\right] \tag{24}$$
$$= C\,\beta(z,\theta)\,T(z,\theta).$$

In general, the backscattering and extinction coefficient can be written

$$\beta(z,\theta) = \beta_0(z)\left[1 + f_\beta(z,\theta)\right], \tag{25}$$

and

$$k_{ext}(z, \theta) = k_0(z) [1 + f_k(z, \theta)], \tag{26}$$

where f_β and f_k are nonnegative and vanish in the absence of horizontal inhomogeneity. If measurement of backscattering and extinction is desired for some altitude z and zenith angle θ_n, then it is clear that the performance of the multiangle lidar could be considerably improved if θ_m, the zenith angle of the second optical path, could be chosen to minimize the effect of horizontal inhomogeneities, i.e., if

$$f_\beta(z, \theta_m) = f_\beta(z, \theta_n) \tag{27a}$$

and

$$f_k(z, \theta_m) = f_k(z, \theta_n) \tag{27b}$$

Then, the transmission coefficient can be determined from

$$T(z, \theta_n) = \left[\frac{F(z, \theta_n)}{F(z, \theta_m)} \right]^{\gamma_{mn}} \tag{28}$$

where

$$\gamma_{mn} = \frac{\cos(\theta_m)}{\cos(\theta_m) - \cos(\theta_n)}. \tag{29}$$

Eqs. (27) cannot be solved simultaneously without additional assumptions. Nevertheless, it is still possible to choose the optimal angular separation between the two optical paths; an algorithm to do so is described below.

1. Lidar returns are obtained at zenith angles $\theta_n = \theta_0 + n\Delta\theta$, where the total range of angles covered should be greater than the angular size of inhomogeneity under consideration. Data collection should include averaging over a number of pulses as well as background measurements to determine the expected value and standard deviation of the backscattered signal. From these data γ_0, the maximum value of γ consistent with the desired accuracy, must be determined using Eq. (23).

2. In the absence of horizontal inhomogeneity

$$\frac{\partial}{\partial \theta} \ln F(z,\theta) = -\frac{2 \tan \theta}{\cos \theta} \int_0^z dz' \, k_{ext}(z') \, . \tag{30}$$

Therefore, for a fixed altitude,

$$G(\theta_n) = \frac{\cos \theta_n}{\tan \theta_n} \frac{F(\theta_n + \Delta\theta) - F(\theta_n - \Delta\theta)}{F(\theta_n)} \approx \text{const.} \tag{31}$$

if the atmosphere is horizontally homogeneous. The homogeneous part of the lidar return can be determined by finding the values of i and j such that

$$|G(\theta_i) - G(\theta_j)| = \min, \quad \text{and } |\gamma_{ij}| \leq \gamma_0 \, . \tag{32}$$

In order to avoid accidental minima, the value of i can be chosen from

$$|G(\theta_i) - G(\theta_{i-1})| + |G(\theta_i) - G(\theta_{i+1})| = \min, \tag{33}$$

in order to ensure that θ_i is in the homogeneous region. Then the appropriate value of j is chosen using Eq. (32). The homogeneous part of the lidar return is given by

$$F_h(z,\theta) = C\beta_h(z)\,[T_h(z)]^{1/\cos\theta} \approx C\beta_0(z)\,[T_0(z)]^{1/\cos\theta} \, , \tag{34}$$

where

$$T_h(z) = [F(z,\theta_i)/F(z,\theta_j)]^{\gamma_{ij} \cos\theta_i}$$

and

$$C\beta_h(z) = F(z,\theta_i)\,[T_h(z)]^{-1/\cos\theta_i}$$

3. The next step requires calculation of the deviation of the measured lidar return from its homogeneou part at (z,θ_n) by determining

$$\Delta F(z,\theta_n) = \ln[F(z,\theta_n)/F_h(z,\theta_n)]$$
$$\approx \ln[1 + f_\beta(z,\theta_n)] - \frac{2}{\cos\theta_n} \int_0^z dz' \, k_0(z') \, f_k(z',\theta_n) \, . \tag{35}$$

Two limiting cases should be considered. In the first case, the measured lidar return is dominated by increased backscattering and $\Delta F > 0$. In this case, condition (27a) can be satisfied if

$$\Delta F(z, \theta_m) = \Delta F(z, \theta_n). \tag{36}$$

In the second case, the measured return is dominated by decreased transmission and $\Delta F < 0$. Therefore, to satisfy condition (27b) one should have

$$\cos \theta_m \, \Delta F(z, \theta_m) = \cos \theta_n \, \Delta F(z, \theta_n). \tag{37}$$

Depending on the sign of ΔF, Eq. (36) or (37) is used in the algorithm described here to determine the optimal angular separation between the optical paths such that $\gamma_{mn} \leq \gamma_0$. Then, the transmission coefficient for each angle is found using Eqs. (28) and (29), subject to the constraint $T(z, \theta_n) \leq T_0(z)^{1/\cos \theta_n}$. If $\Delta F \approx 0$, then the transmission coefficient along that LOS is the same as in the homogeneous case. If ΔF has an extremum for some value of θ_n, so that Eq. (36) or (37) cannot be satisfied, then

$$T(z, \theta_n) = \left[\frac{F(z, \theta_{n+i})}{F(z, \theta_{n-j})} \right]^{\gamma_{ex}}, \tag{38}$$

where

$$\gamma_{ex} = \frac{\cos(\theta_{n+i}) \cos(\theta_{n-j})}{\cos(\theta_n) \left[\cos(\theta_{n-j}) - \cos(\theta_{n+i}) \right]} \leq \gamma_0. \tag{39}$$

The values i and j in Eqs. (38) and (39) can be found, for example, as follows. For $j = 1$ find the value of i such that either Eq. (36) or (37) is satisfied, subject to the constraint given by Eq. (39). If this value of i is greater than some specified maximum value (10 was used in the calculations described here) then the process is repeated with increasing values of j until all of the above conditions are satisfied.

In the presence of a horizontal inhomogeneity of finite extent in altitude, say from z_0 to z_1, the algorithm is expected to perform best for $z \leq z_0$ and $z \geq z_1$. The worst performance may be expected if the change in lidar return due to increased backscattering is nearly compensated by decreased transmission.

Another source of error may be due to the finite angular spacing between the optical paths used. The return at the optimal value of the zenith angle may not be available. This may be especially important for inhomogeneities of small angular size.

4. Model Calculations

Algorithm performance was tested on two simple models of horizontal inhomogeneities:
(A) A Gaussian model of inhomogeneity

$$f(\theta) = \begin{cases} \exp\left[-(\theta - \theta_c)^2/2\theta_w^2\right], & z_0 \leq z \leq z_1 \\ 0, & \text{otherwise} \end{cases} \tag{40}$$

(B) A double Gaussian model of asymmetric inhomogeneity with structure on smaller angular scale

$$f(\theta) = \begin{cases} \exp\left[-(\theta - \theta_c)^2/2\theta_w^2\right] + 0.5 \exp\left[-(\theta - \theta_c + 4\theta_w)^2/2\theta_w^2\right], & z_0 \leq z \leq z_1 \\ 0, & \text{otherwise} \end{cases} \tag{41}$$

In order to reduce the numbers of arbitrary parameters, it is assumed here that $f_\beta(z, \theta) = A_\beta f(\theta)$ and $f_k(z, \theta) = A_k f(\theta)$. It is important to note that this simplification does not affect the performance of the algorithm, since it does not rely on any prior information about the structure of the inhomogeneous region, which is usually unavailable during measurements.

For the horizontal inhomogeneity extending in altitude from z_0 to z_1, let $T_0(z) = \exp[-\int_0^z dz' \, k_0(z')]$ and $T_1(z) = \exp[-\int_{z_0}^z dz' \, k_0(z')]$. Then, Eq. (24) may be written as

$$F(z, \theta) = \beta(z)[1 + A_\beta f(\theta)] \, T_0(z)^{1/\cos\theta} \, T_1(z)^{A_k f(\theta)/\cos\theta}. \tag{42}$$

The following cases were considered: (1) below inhomogeneity; (2) at the lower edge of inhomogeneity; (3) and (4) inside inhomogeneity; and (5) above inhomogeneity. Suppose that a sufficient number of pulses is used for signal averaging so that the relative error in transmission coefficient from Eq. (23) is less than 1% for $\gamma_0 = 15$. Then, the expected

lidar signal for the two models is shown in Figs. 1 and 2. It is seen that at the lower edge of inhomogeneity (case 2) the signal is dominated by the increase in backscattering; in case 4 the increase in backscattering is almost completely compensated by decrease in transmission coefficient; while in case 5 the signal is dominated by reduced transmission. The performance of the algorithm for these lidar signals is illustrated in Figs. 3-4 and 5-6, where, irrespective of the sampling interval used, the calculated transmission coefficient is shown at intervals of 5° to avoid symbol overcrowding. As expected, the performance is the worst for case 4 where the lidar signal closely resembles that of homogeneous atmosphere. The performance is very good at both the lower and upper edges of the inhomogeneity, indicating that this method can provide accurate data on transmission through inhomogeneities such as clouds, provided they are not optically thick. This conclusion appears to be independent of the shape and nature of inhomogeneity; the results are equally good for both models. The accuracy does depend on the sampling interval $\Delta\theta$ used during measurements. Not surprisingly, comparison between Figs. 3-4 and 5-6 indicates that more complex structures of inhomogeneity require finer sampling intervals. For a given sampling interval, the accuracy does not depend strongly on the value of γ_0, provided it is chosen to allow the use of neighboring optical paths to determine the transmission coefficient.

5. Conclusions

The performance of the single-ended multiangle lidar for real-time measurements of atmospheric properties was analyzed in the presence of signal-induced shot noise and horizontal inhomogeneities in atmospheric extinction and backscattering. Noise considerations lead to the minimum angular separation between the optical paths (based on signal and background levels, and on number of pulses used for signal averaging) needed to determine the transmission coefficient with a desired accuracy from the range-resolved lidar returns. A simple algorithm to determine the transmission coefficient to a given altitude in a horizontally inhomogeneous region was described. This algorithm makes no *ad hoc*

assumptions about the relationship between the backscattering and extinction coefficients, and does not require a priori knowledge about the structure of inhomogeneities. While this algorithm does not perform very well inside a horizontal inhomogeneity, it can determine the overall transmission of optically thin inhomogeneities with high accuracy.
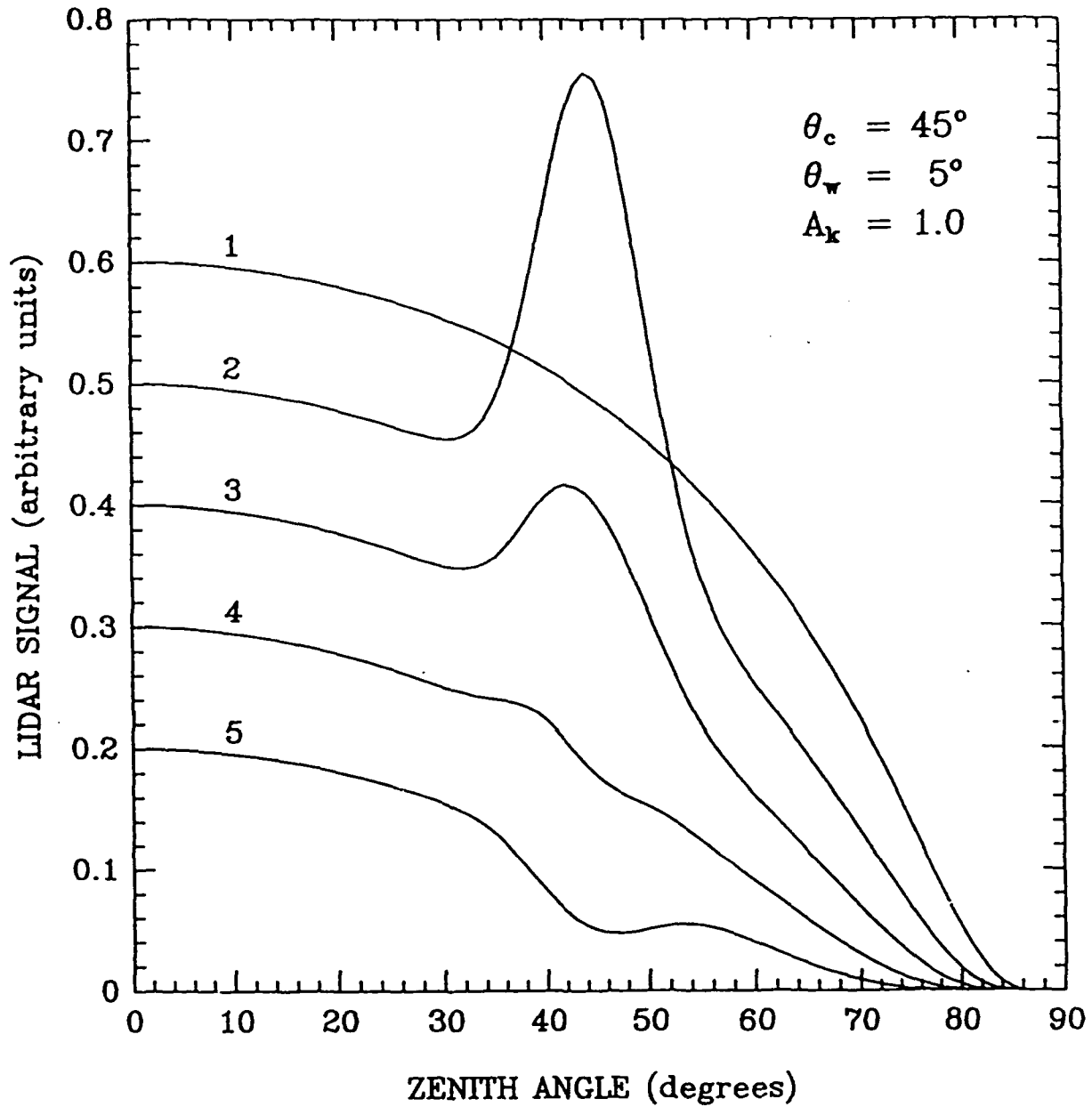
Fig. 1. Expected lidar return for a model A of horizontal inhomogeneity (Eq. (23)):

    (1) below inhomogemeity ($T_0 = 0.6$, $T_1 = 1.0$, $A_\beta = 0.$);

    (2) at the lower edge of inhomogeneity ($T_0 = 0.5$, $T_1 = 1.0$, $A_\beta = 1.$);

    (3) inside inhomogeneity ($T_0 = 0.4$, $T_1 = 0.8$, $A_\beta = 1.$);

    (4) inside inhomogeneity ($T_0 = 0.3$, $T_1 = 0.6$, $A_\beta = 1.$);

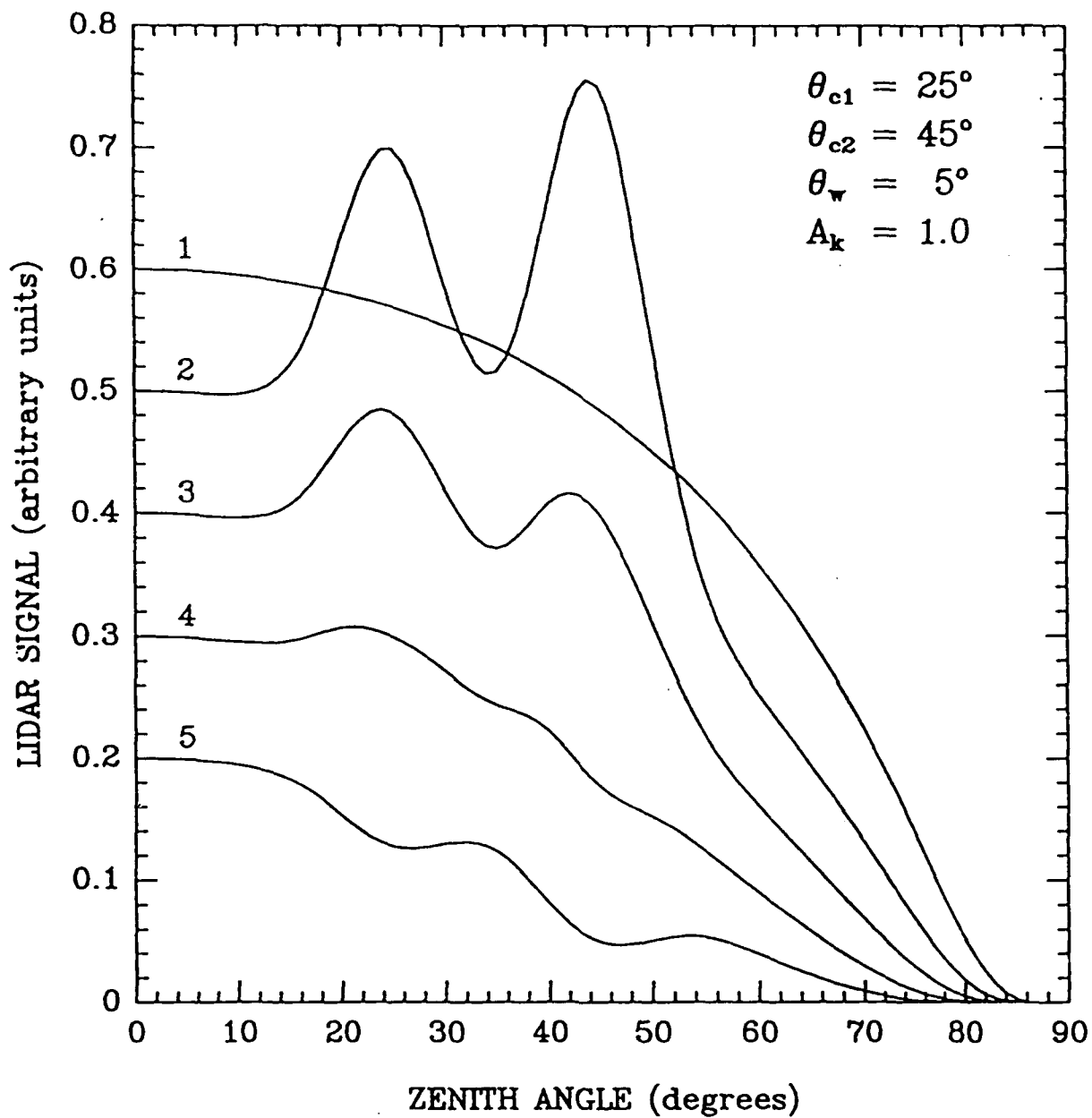   (5) above inhomogeneity ($T_0 = 0.2$, $T_1 = 0.6$, $A_\beta = 0.$).

Fig. 2. Expected lidar return for a model B of horizontal inhomogeneity (Eq. (24)); different cases are defined in Fig. 1.
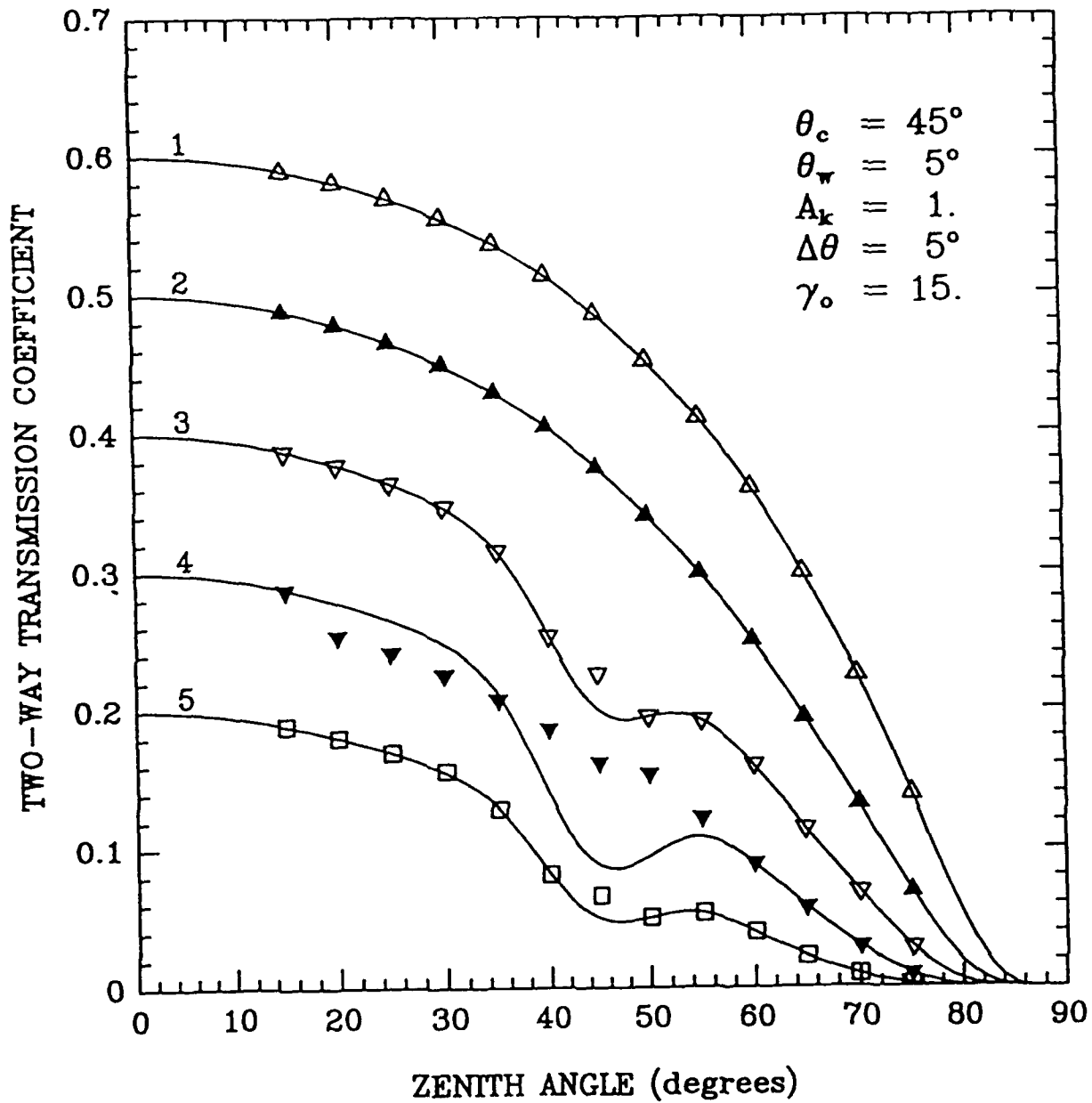
Fig. 3. Algorithm performance for model A of horizontal inhomogeneity with $\Delta\theta = 5°$; different cases are defined in Fig. 1.
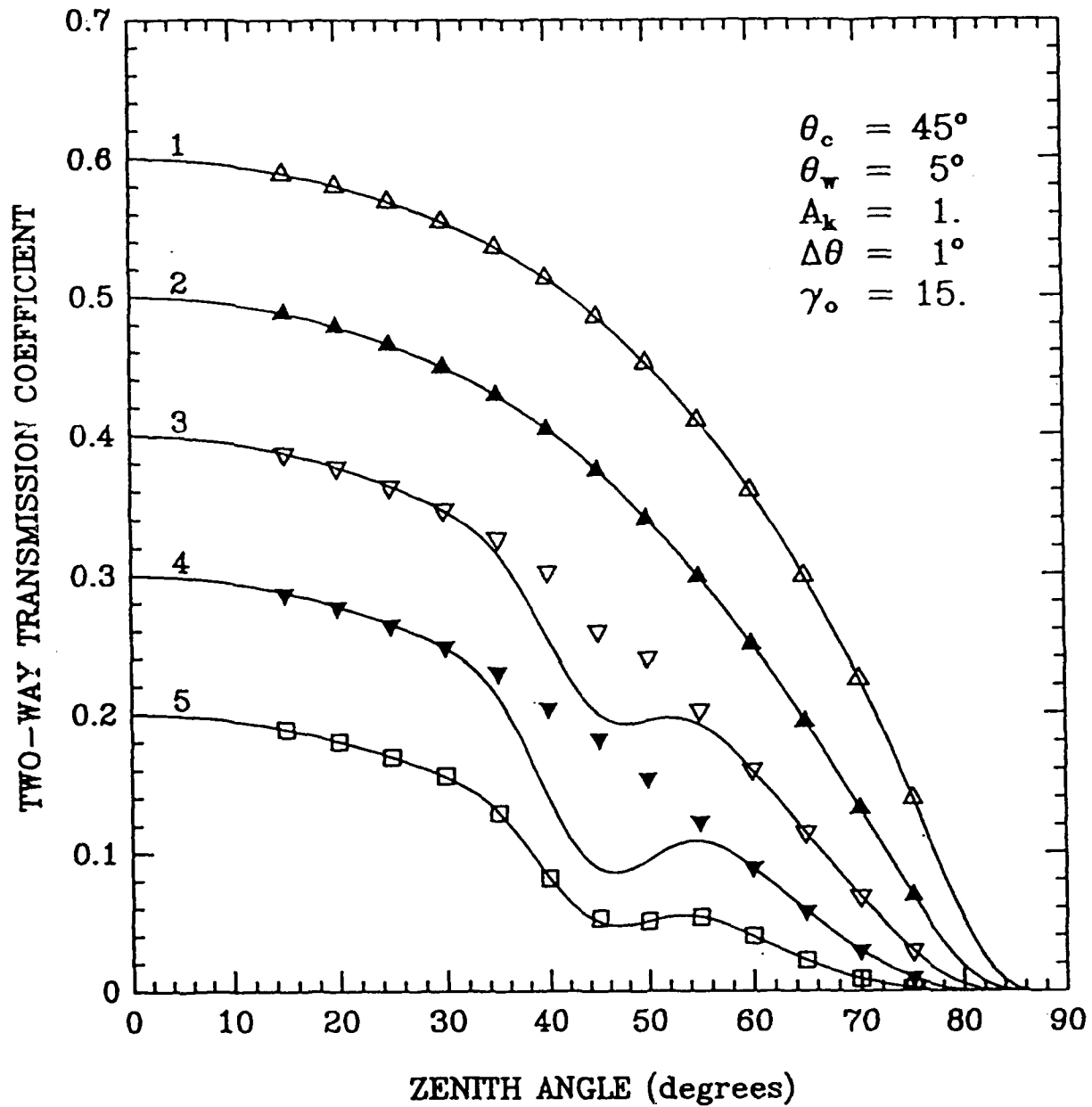
Fig. 4. Algorithm performance for model A of horizontal inhomogeneity with $\Delta\theta = 1°$; different cases are defined in Fig. 1.
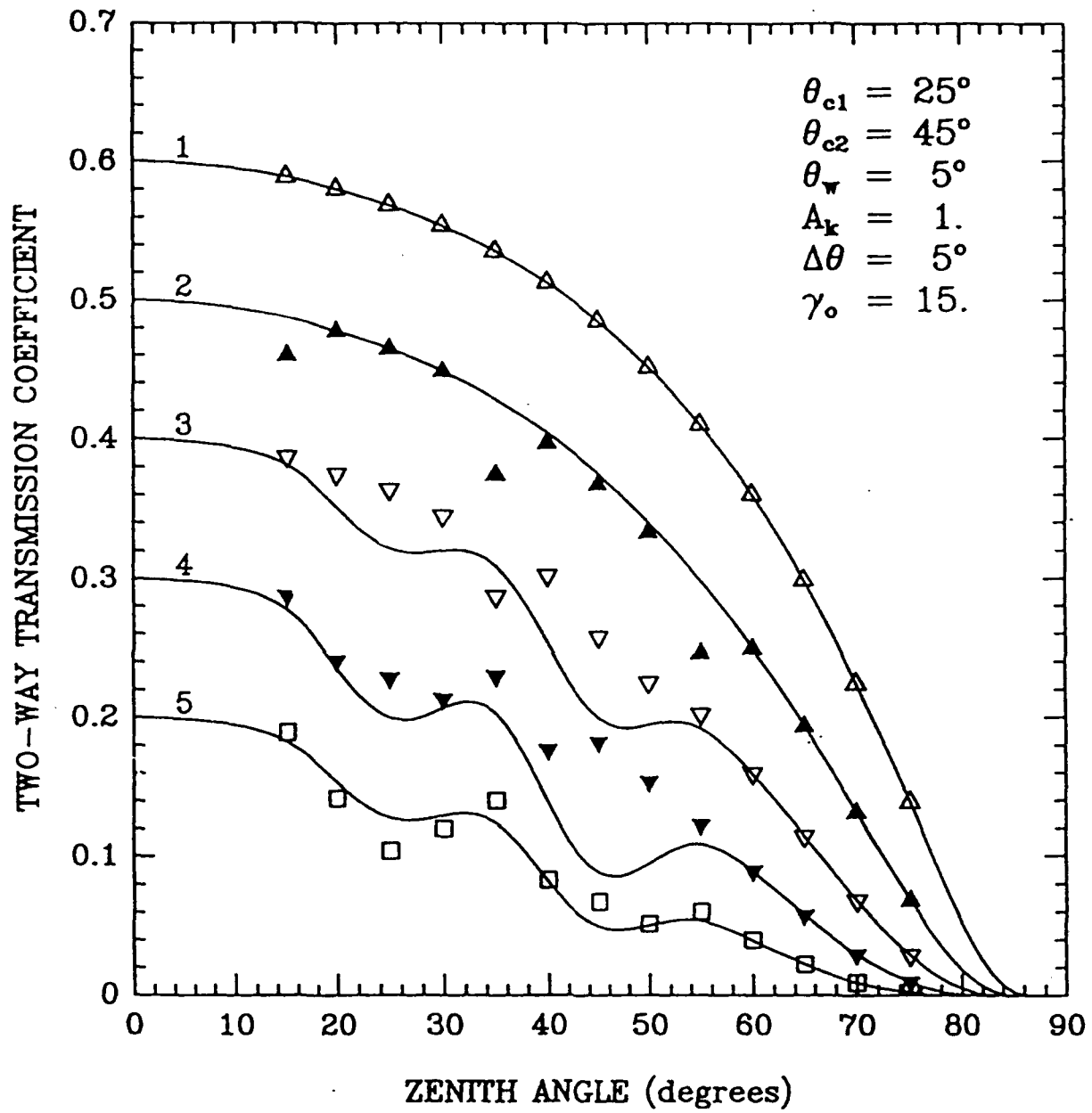
Fig. 5. Algorithm performance for model B of horizontal inhomogeneity with $\Delta\theta = 5°$; different cases are defined in Fig. 1.

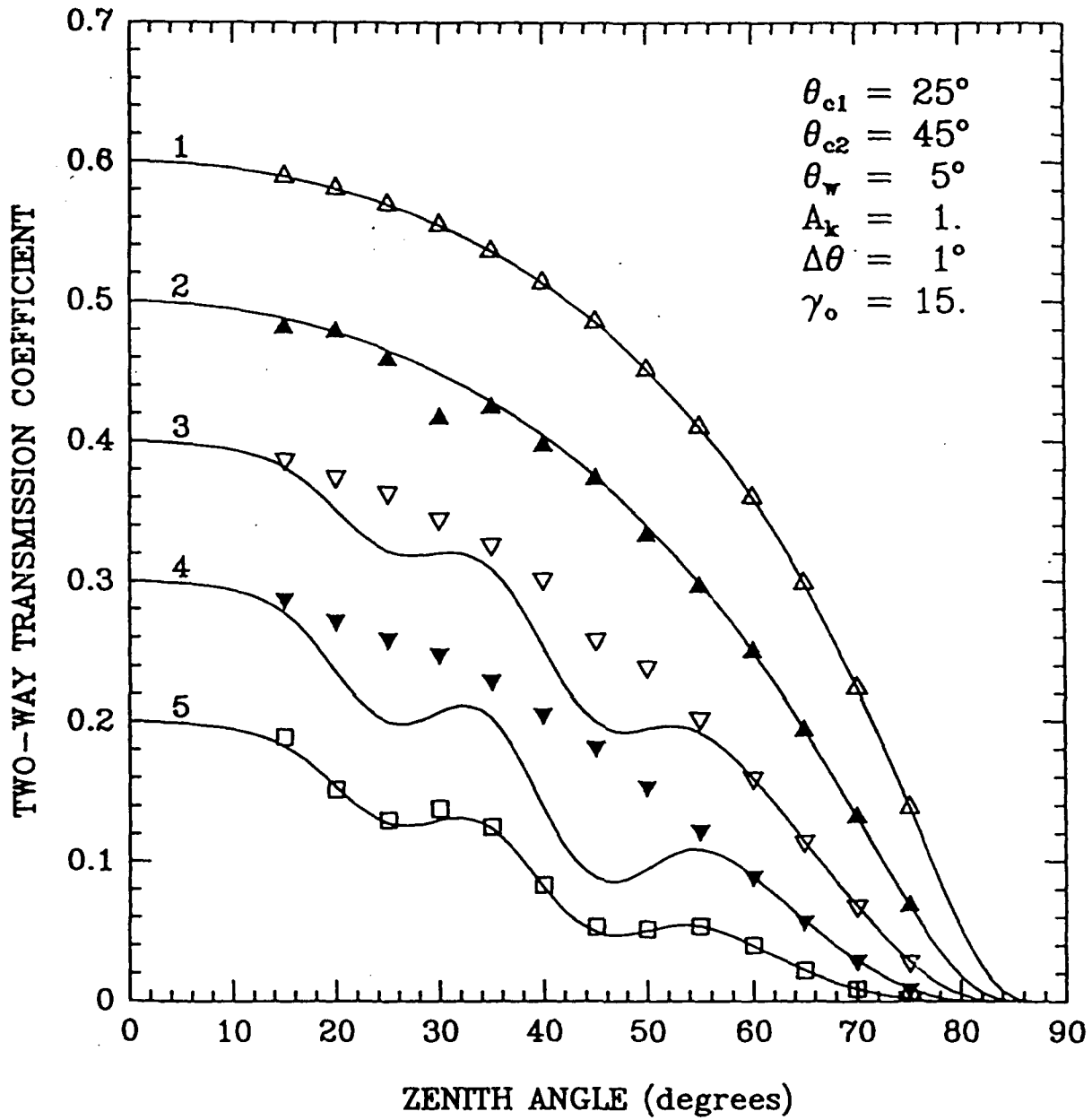Fig. 6. Algorithm performance for model B of horizontal inhomogeneity with $\Delta\theta = 1°$; different cases are defined in Fig. 1.

References

1. R. M. Measures, *Laser Remote Sensing*, Wiley, New York, 1984.

2. S. T. Shipley, D. H. Tracey, E. W. Eloranta, J. T. Trauger, J. T. Sroga, F. L. Roesler, and J. A. Weinman, "High Spectral Resolution Lidar to Measure Optical Scattering Properties of Atmospheric Aerosols. 1: Theory and Instrumentation", Appl. Opt., **22**, 3716-3724 (1983).

3. J. T. Sroga, E. W. Eloranta, S. T. Shipley, F. L. Roesler, and P. J. Tryon, "High Spectral Resolution Lidar to Measure Optical Scattering Properties of Atmospheric Aerosols. 2: Calibration and Data Analysis", Appl. Opt., **22**, 3725-3732 (1983).

4. G. J. Kunz, "Bipath Method as a Way to Measure the Spatial Backscatter and Extinction Coefficients with Lidar", Appl. Opt., **26**, 794-795 (1987).

5. H. G. Hughes and M. R. Paulson, "Double-Ended Lidar Technique for Aerosol Studies", Appl. Opt., **27**, 2273-2278 (1988).

6. J. D. Spinhirne, J. A. Reagan, and B. M. Herman, "Vertical Distribution of Aerosol Extinction Cross Section and Inference of Aerosol Imaginary Index in the Troposphere by Lidar Technique", J. Appl. Meteor., **19**, 426-438 (1980).

7. M. R. Paulson, "Atmospheric Horizontal-Inhomogeneity Effects on the Optical Depths Determined by the Double-Evaluation-Angle Lidar Technique", Report TD 1600, DTIC AD-a212 836, NOSC, 1989

8. M. C. W. Sandford, "Laser Scatter Measurements in the Mesosphere and Above", J. Atmos. Terr. Phys., **29**, 1657-1662 (1967).

9. H. Shimizu, Y. Sasano, H. Nakane, N. Sugimoto, I, Matsui, and N. Takeuchi, "Large Scale Laser Radar for Measuring Aerosol Distribution Over a Wide Area", Appl. Opt., **24**, 617-626 (1985).

10. J. D. Klett, "Stable Analytical Inversion Solution for Processing Lidar Returns", Appl. Opt., **20**, 211 (1981).

11. J. D. Klett, "Lidar Inversion with Variable Backscatter Extinction Ratios", Appl. Opt., **24**, 1638 (1985).

12. W. Feller, *An Introduction to Probability Theory and Its Applications*, Wiley, New York, 1970.